# Evidence for Hydrophobic Interaction between Galanin and the GalR1 Galanin Receptor and GalR1-Mediated Ligand Internalization: Fluorescent Probing with a Fluorescein−Galanin

Suke Wang,* Anthony Clemmons, Catherine Strader, and Marvin Bayne

*Department of CNS/CV Biological Research, Schering-Plough Research Institute, 2015 Galloping Hill Road, Kenilworth, New Jersey 07033*

*Received December 31, 1997; Revised Manuscript Received April 22, 1998*

ABSTRACT: Galanin is a neuropeptide that activates specific receptors to modulate several physiological functions including food intake, nociception, and learning and memory. The molecular nature of the interaction between galanin and its receptors and the fate of the galanin/receptor complex after the binding event are not understood. A fluorescein−N-galanin (F−Gal) was generated to measure the interaction between galanin and rat GalR1 galanin receptor (rGalR1) and rGalR1-mediated ligand internalization using flow cytometry in transfected Chinese hamster ovary (CHO) cells. Like galanin, F−Gal bound rGalR1 with high affinity and stimulated intracellular signaling events. Fluorescence quenching by soluble KI of rGalR1-bound F−Gal revealed a highly protected environment around the fluorescein, suggesting that the N-terminal portion of galanin, which constitutes the binding site of galanin for the receptor, binds to a protected hydrophobic binding pocket within the receptor. Exposure to F−Gal stimulated rapid ($t_{1/2}$ ∼10 min) and extensive (78%) internalization of surface F−Gal into rGalR1/CHO cells at 37 °C but not at 0 °C. In addition, the internalization did not occur in parental CHO cells at either 0 or 37 °C and was inhibited by addition of 0.25 M sucrose in the medium, indicating a GalR1-mediated energy-requiring endocytic process. These results revealed a hydrophobic interaction between galanin and the GalR1 receptor, which is in contrast to those of other G protein-coupled receptors that mainly require hydrophilic interaction with their peptide ligands near or outside the plasma membrane surface, and illustrated that the initial binding interaction is followed by rapid cellular internalization of the agonist/GalR1 complex.

The neuropeptide galanin is a pleiotropic hormone that regulates several important physiological functions in the digestive, endocrine, and central nervous systems (*1*−*3*). In the digestive systems, galanin modulates smooth muscle contraction and the release of gastrin and gastric acid; in the endocrine systems, galanin regulates the release and secretion of hormones such as insulin; and in the central nervous system, it modulates nociception and feeding behavior as well as controlling the release of acetylcholine, dopamine, and prolactin (*4*−*7*).

The actions of galanin are mediated through specific receptors. Recent molecular cloning and characterization of galanin receptors have greatly enhanced our understanding of galanin biology. Three galanin receptor subtypes, GalR1, GalR2, and GalR3, have been cloned and share a mere 36−54% homology (*8*−*10*). All three receptors are members of the G protein-coupled receptor (GPCR)[1] superfamily characterized by seven hydrophobic transmembrane domains (TMs) (11). Upon activation by agonists, these receptors mediate G protein-coupled intracellular signaling via second message pathways, such as inhibition of forskolin-stimulated cAMP production. The coding region of the GalR1 gene consists of three exons and two introns, with the second exon encoding exclusively the third intracellular loop (*12*). Rat galanin is a 29 amino acid peptide with amidation at the C-terminus, whereas human galanin consists of 30 amino acids without C-terminal amidation. The ligand-binding profiles of the three receptors are distinguished by their differential affinities for galanin(2−29), which lacks the N-terminal G residue of galanin, and for galanin(1−16), which lacks the 13 residues of the C-terminus of galanin. Galanin(2−29) binds to GalR2 and GalR3 with high affinity but the affinity for GalR1 is significantly lower (*10*, *13*). In contrast, galanin(1−16) binds to GalR1 and GalR2 with high affinity but its affinity for GalR3 is significantly lower (*10*). In solution, galanin adapts a "horseshoe" conformation with residue P13 serving as a potential β-bend (*14*). The sequence of amino acids 1−15 of galanin is identical across several species and appears to form an α-helical structure (*14*), consistent with a role in receptor interaction. In contrast, truncation or replacement of the C-terminal portion beyond amino acid 16 or 13 resulted in no significant loss of receptor binding, suggesting that this region of the peptide is not critical for interacting with the receptors (*10*, *15*).

Despite the cloning and pharmacological characterization of the three galanin receptor subtypes, little is known about the nature of the interaction between galanin and its receptors and about the cellular events for the ligand/receptor complex

* Corresponding author: Tel (908) 298-3949; FAX (908) 298-2383; E-mail suke.wang@spcorp.com.

[1] Abbreviations: GPCR, G protein-coupled receptor; TM, transmembrane domain; DMEM, Dulbecco's modified Eagle's medium; PBS, phosphate-buffered saline; PMSF, phenylmethanesulfonyl floride; FCS, fetal calf serum; rGalR1, rat type I galanin receptor; F−Gal, fluorescein-labeled rat galanin; CHO, Chinese hamster ovary; OAG, 1-oleoyl-2-acetyl-*sn*-glycerol; SPA, scintillation proximity assay; HPLC, high-performance liquid chromatography.

S0006-2960(97)03195-4 CCC: $15.00 
Published on Web 06/11/1998

after the ligand binds to the receptors. To address these questions regarding the molecular nature of galanin/GalR1 receptor interaction and agonist-induced internalization of galanin, we have generated a fluorescent, N-terminally labeled fluorescein−galanin (F−Gal) and a Chinese hamster ovary (CHO) cell line stably expressing rat GalR1 receptor. Using flow cytometric measurements, we have found that F−Gal binds to the GalR1 receptor in a protected, highly hydrophobic environment and that this binding leads to rapid internalization of the fluorescent galanin mediated by the GalR1 receptor.

## MATERIALS AND METHODS

*Materials.* Porcine $^{125}$I-galanin (2200 Ci/mmol) was purchased from DuPont−NEN (Boston, MA). Rat galanin (MW 3163) and biotinyl-rat galanin (catalog no. 7234, MW 3389) were purchased from Peninsula Laboratories, and quality controls of biotinyl-galanin were performed with thin-layer chromatography, amino acid analysis, and HPLC analysis (Peninsula Laboratories, Belmont, CA). F−Gal was custom-synthesized by reacting the isothiocyanate group of fluorescein isothiocyanate (FITC, MW 390) with the free amino group at the N-terminus of rat galanin to form a thiourea bond between the label and galanin (Figure 1A) (Genosis Biotechnology, The Woodlands, TX). F−Gal was purified and characterized with HPLC (VYDAC RP C8 column, 10−90% acetonitrile, 34 min) and mass spectroscopy by the manufacturer. 5-(Dodecanoylamino)fluorescein was from Molecular Probes, Inc. (Eugene, OR). Fluorescein−streptavidin was purchased from Fisher Scientific (Pittsburgh, PA).

*Generation of Stable CHO Cell Line Expressing Rat GalR1 Receptor*. Rat GalR1 receptor cDNA (GenBank accession number U30290) was generated by reverse transcriptase−polymerase chain reaction with rat hypothalamus total RNA as template. The sequence was confirmed by DNA sequencing and cloned into mammalian expression vector pCR3. CHO cells grown in F12 medium/10% FCS were transfected with the plasmid pCR3-rGalR1 by electroporation, and a cell line that expresses rGalR1 (rGalR1/CHO) was clonally selected in the presence of Geneticin (G418, 500 $\mu$g/mL). Radioligand binding assays performed with $^{125}$I-galanin as ligand and membranes prepared from rGalR1/CHO showed a $K_D$ of 0.2 nM and a $B_{max}$ of 350 fmol/mg of protein, which represents approximately 20 000 receptors/cell. A mock-transfected CHO line (pCR3 alone) was similarly selected and, like the parental CHO cells, showed no detectable [$^{125}$I]galanin binding to its membrane preparation.

*Fluorescence Spectroscopy*. Emission and excitation spectra of F−Gal (1 $\mu$M) in PBS without $Ca^{2+}$/$Mg^{2+}$/ plus 0.1% BSA (w/v) were measured in a Spex Fluorolog-2 fluorometer (Spex Industries Inc., Edison, NJ) at room temperature with 1 s integration time at each wavelength (nanometers). The emission spectrum was scanned between 470 and 600 nm with an excitation wavelength of 440 nm and the excitation spectrum was taken between 400 and 520 nm with an emission wavelength of 550 nm. For both emission and excitation spectra, the background counts (buffer alone) were less than 2% of the peak intensities of F−Gal and were subtracted. In KI quenching experiments,

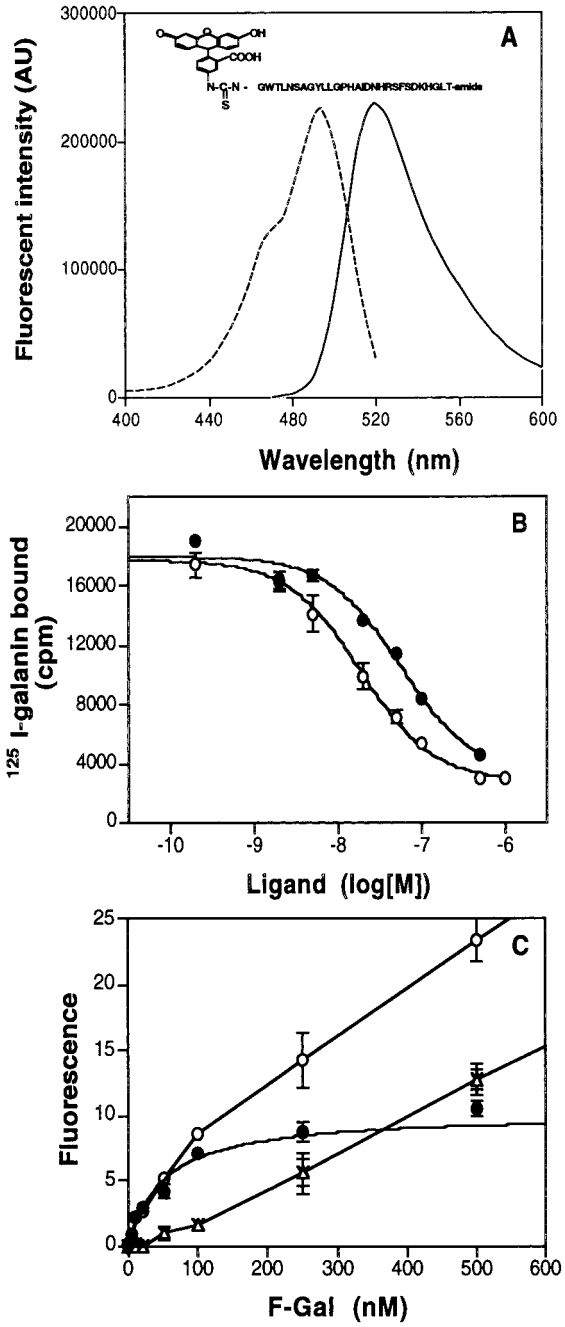


FIGURE 1: Functional analysis of F−Gal. (A) Structure and corrected excitation (- - -) and emission (—) spectra of F−Gal. The left portion of the structure is fluorescein and on the right portion is the amino acid sequence of rat galanin starting at residue Gly (G) and ending with an amide at the C-terminus. The spectra were measured with 1 $\mu$M F−Gal in PBS without $Ca^{2+}$/$Mg^{2+}$, containing 0.1% BSA (w/v). Background fluorescence (buffer alone) for both excitation and emission (<2%) was subtracted. AU, arbitrary units. (B) Competition binding of [$^{125}$I]galanin with galanin (○) and F−Gal (●) for rGalR1/CHO cells. Data were analyzed by a nonlinear regression method to fit one-site competition curves (mean ± SE, $n$ = 3). (C) Direct binding of F−Gal to rGalR1 determined by flow cytometry. Rat GalR1/CHO or CHO cells ($2 \times 10^5$) were incubated at various concentrations of F−Gal for 1 h at 0 °C and analyzed with flow cytometry. Autofluorescence (7.02 ± 0.10, $n$ = 3) was subtracted from the data points. Specific binding (●) is the fluorescence calculated as the mean fluorescence of total binding (○) minus that of nonspecific binding (Δ) defined by using 5 $\mu$M unlabeled galanin in the incubation. Symbol (×) denotes nonspecific binding of F−Gal to CHO cell. Data represent means ± SD ($n$ = 3) and the curve for specific binding (●) shows the best fit of nonlinear regression.

emission intensity of free F−Gal (0.5 $\mu$M) in PBS plus 0.1% BSA (w/v) was similarly determined between 470 and 600 nm with an excitation at 440 nm at intervals of 1 nm with 0.5 s integration time at each wavelength. The fluorescent intensities, calculated by integration, within the emission range minus the intensities of buffer alone at appropriate KI concentrations were used to calculate quenching.

*Radioligand Binding Assays.* In whole-cell binding assays, cells were washed with PBS and scraped off plates. Half a million cells were incubated with 0.1 nM porcine $^{125}$I-galanin in the presence of various concentrations of peptide ligands. The incubation proceeded for 1 h at room temperature in 100 $\mu$L of buffer A [PBS without $Ca^{2+}/Mg^{2+}$, plus 0.1% BSA (w/v) and 0.01% $NaN_3$] and was terminated by rapid vacuum filtration through Multiscreen FB Filter Plates (Millipore, Bedford, MA) presoaked with 0.3% poly(ethylenimine) (pH 7.4). The filters were washed three times with 100 $\mu$L of cold PBS and counted with a MicroBeta counter (Pharmacia, NJ). Membranes from rGalR1/CHO cells and from COS-7 cells transiently transfected with rat GalR1 cDNA were prepared as described previously (*13*). Radioligand binding assays with cellular membranes were performed by incubating 10 $\mu$g of membrane proteins in 100 $\mu$L of buffer consisting of 25 mM Tris-HCl, pH 7.4, 0.1% BSA (w/v), 0.1% bacitracin, 10 mM $MgCl_2$, 50 $\mu$M PMSF, 5 $\mu$g/mL aprotinin, and 0.5 mM EDTA, for 1 h at room temperature, followed by filtration as described above.

*Measurement of Intracellular cAMP Production.* rGalR1/CHO cells at 90% confluence were washed with PBS and scraped off plates. The cells were centrifuged and resuspended in buffer B (75 mM Tris-HCl, pH 7.4, 250 mM sucrose, 12.5 mM $MgCl_2$, 1.5 mM EDTA, 0.2 mM sodium metabisulfite, and 0.2 mM 3-isobutyl-1-methylxanthine) at $2 \times 10^5$ cells/100 $\mu$L. Rat galanin or F−Gal (20 $\mu$L) at 0.05, 0.5, 5, 50, 500, 5000, and 50 000 nM and 10 $\mu$L of forskolin (1.3 mM in 10% DMSO) in buffer B were added to the cells. The mix was incubated at room temperature for 45 min with vigorous shaking (210 rpm) followed by boiling for 3 min. The cell lysates were stored at −20 °C until assay for cAMP. The cAMP contents in 20 $\mu$L of the cell lysates were determined using a cAMP scintillation proximity assay kit (cAMP SPA, catalog no. RPA 556, Amersham, Arlington Heights, IL).

*Flow Cytometry.* CHO or rGalR1/CHO cells grown just to confluence were briefly trypsinized off plates, washed with PBS, and resuspended in buffer C [PBS without $Ca^{2+}/Mg^{2+}$ plus 0.1% BSA (w/v)]. The cells were incubated with F−Gal in a total volume of 100 $\mu$L and analyzed with a FACScan flow cytometer (Becton Dickinson Immunocytometry Systems, Inc.) immediately after addition of 0.5 mL of cold buffer C. Instrumental setting at FL1 for measurements of fluorescein fluorescence (laser excitation at 488 nm and emission at 515 nm, bandwidth 30 nm) was utilized in the analysis. Live cells were gated by light scattering or by exclusion of propidium iodide, and 100 000 events were acquired in each scan. When fluorescein-labeled fatty acid, 5-dodecanoylaminofluorescein (F−FA), was used, only live and stained cells were gated for measurements. Mean fluorescent intensity of gated cells, minus the mean fluorescence of blank cells (autofluorescence) or, in the case of KI quenching, minus the mean fluorescence of CHO cells (without GalR1) incubated with 100 nM F−Gal at appropriate KI concentrations, was used as the net intensity for calculations (*16*). The concentrations of KI used in the quenching experiments did not cause a noticeable change of cell sizes. Cellular lysis was observed only when [KI] was larger than 0.35 M.

*Internalization Studies.* F−Gal (100 nM) was incubated with rGalR1/CHO or CHO cells in 100 $\mu$L of buffer C at 0 or 37 °C for designated time. At the end of incubation, the stained cells were either incubated with 0.5 mL of buffer A containing either 0 $\mu$M (to obtain fluorescence of total binding, including the surface and internalized F−Gal) or 5 $\mu$M unlabeled galanin (to obtain fluorescence of internalized F−Gal in the presence of the competing galanin) at 0 °C for 45 min. The difference between the total and internalized F−Gal represented the surface-bound F−Gal. The postincubation with 5 $\mu$M unlabeled galanin to remove the cell surface F−Gal was also tested for 30 and 75 min. Like the 45-min postincubation, these incubations also removed the surface F−Gal, suggesting longer competition time was not necessary. The fluorescent intensities of the cells were measured by cell flow cytometry as described above.

*Data Analysis.* DNA sequencing data, obtained by using the fluorescent dye termination method (Perkin-Elmer, Branchburg, NJ) on an automated DNA sequencer (Model 373, Applied Biosystems, Inc.), were analyzed with the DNA* software package (DNAstar, Inc. Madison, WI). KI fluorescence quenching data were analyzed according to

$$F_o/F = K_q\,[\mathrm{KI}] \qquad (1)$$

where [KI] is the molar concentration of the quencher, $K_q$ is the quenching constant, and $F_o$ and $F$ are the fluorescent intensities at [KI] = 0 or the appropriate molar concentration of [KI], respectively (*17*). The radioligand competition and cyclic AMP data were analyzed by one-site competition of nonlinear regression, while the data of F−Gal saturation binding on rGalR1/CHO cells were analyzed by one-site hyperbolic binding of nonlinear regression using the Prism GraphPad software (San Diego, CA).

## RESULTS AND DISCUSSION

*Optical and Functional Characterization of F−Gal.* The fluorescein-labeled galanin (F−Gal) had the expected molecular weight of 3640, representing the sum of one molecule of fluorescein and one molecule of galanin (fluorescein:galanin = 1:1) and a purity of 98.7% as analyzed by mass spectroscopy and HPLC, respectively. Optical properties of F−Gal were analyzed by excitation, emission, and absorption spectra. The excitation spectrum was scanned between 400 and 520 nm and displayed a major peak with a maximum intensity at 493 nm accompanied by a small shoulder at 465 nm (Figure 1A). The emission spectrum was scanned between 470 and 600 nM and displayed a single peak at 519 nm (Figure 1A). The absorption spectrum was similar to the excitation spectrum in the same wavelength range (not shown). The spectra closely resemble typical optical properties of fluorescein conjugates (*18*), indicating well-preserved chemical and optical characteristics during the labeling reactions. The relative fluorescence of F−Gal was 0.3 times that of free FITC. The yield is consistent with the observations that fluorescence of fluorescein and most other dyes is typically decreased by >50% upon conjugation (*33*).

Table 1: Functional Characterization of F−Gal and Biotinyl-galanin

| assay | ligand | affinity/ potency | relative affinity/ potency[a] |
|---|---|---|---|
| (A) Radioligand Binding [$K_i$[b] (nM)] | | | |
| rGalR1/CHO/whole-cell | galanin | 14 ± 3 (3) | 1 |
| | F−Gal | 46 ± 9 (3) | 3.2 |
| rGalR1/COS-7/membrane[c] | galanin | 0.10 ± 0.02 (3) | 1 |
| | F−Gal | 1.17 ± 0.16 (3) | 11.7 |
| | biotinyl-galanin | 0.3 ± 0.2 (3) | 3 |
| rGalR1/CHO/membrane | galanin | 0.07 ± 0.02 (3) | 1 |
| | biotinyl-galanin | 0.4 ± 0.07 (3) | 6.25 |
| (B) Flow Cytometry [$K_D$ (nM)] | | | |
| rGalR1/CHO/whole-cell | F−Gal | 49 ± 13 (3) | N/A[d] |
| (C) Cyclic AMP[e] [$EC_{50}$ (nM)] | | | |
| rGalR1/CHO/whole-cell | galanin | 6.2 ± 2.1 (2) | 1 |
| | F−Gal | 10.4 ± 4.7 (2) | 1.7 |

[a] Relative affinity/potency values as compared with that of the galanin in each type of assays. [b] $K_i$ values in the competition assays were calculated by using the $IC_{50}$ values determined by nonlinear regression analysis of the data ($K_i = IC_{50}/(1 + ([^{125}I\text{-galanin}]/K_D))$ where [$^{125}$I-galanin] is the concentration of the radioligand used in the assay and $K_D$ is the dissociation constant of $^{125}$I-galanin (*32*). [c] Rat GalR1 receptor was expressed by transiently transfecting COS-7 cells by electroporation with plasmid pCR3-rGalR1. The expression levels in the COS-7 cells were about 700 fmol/mg of membrane proteins. [d] N/A, not applicable. [e] Intracellular cAMP in rGalR1/CHO cells was stimulated in the presence of 0.1 mM forskolin. Concentrations of galanin or F−Gal used were 0, 0.005, 0.05, 0.5, 5, 50, 500, and 5000 nM. At the end of incubation the cells were lysed and cellular cAMP was determined with SPA. The basal and forskolin-stimulated cAMP levels were 6.1 ± 1.3 pmol/$10^6$ cells ($n = 4$) and 564 ± 17 pmol/$10^6$ cells ($n = 4$), respectively.

The functional properties of F−Gal were analyzed in (1) radioligand competition assays with intact CHO cells expressing rGalR1 and with membrane preparations from COS-7 cells transiently transfected with rGalR1 cDNA; (2) functional assays for inhibition of forskolin-stimulated cAMP production in rGalR1/CHO cells; and 3) saturation binding of F−Gal to rGalR1/CHO cells measured with flow cytometry. In the radioligand competition assays with intact rGalR1/CHO cells, both rat galanin and F−Gal competed with $^{125}$I-galanin with high affinity ($K_i$ of 14 nM vs 46 nM for galanin and F−Gal; Figure 1B and Table 1). When the competition assays were performed with isolated membranes prepared from COS-7 cells expressing the rGalR1 receptor, comparably high affinities were also observed for galanin and F−Gal, i.e., 0.10 nM for galanin and 1.17 nM for F−Gal (Table 1).

To determine whether the addition of fluorescein affected the ability of galanin to activate its receptor, the effect of F−Gal on rGalR1-mediated inhibition of forskolin-stimulated intracellular cAMP production was measured. In these experiments, rGalR1/CHO cells were incubated with galanin or F−Gal at concentrations up to 5 $\mu$M in the presence of 0.1 mM forskolin. Both galanin and F−Gal inhibited forskolin-induced cAMP production in a dose-dependent fashion. Nonlinear regression analysis yielded $EC_{50}$ values of 6.2 ± 2.1 and 10.4 ± 4.7 nM and maximum inhibition of 66% ± 5% and 65% ± 6% for galanin and F−Gal, respectively (Table 1). The data demonstrate that, like galanin, F−Gal is capable of activating the galanin receptor for signal transduction.

Direct saturation binding of F−Gal to rGalR1 receptor on rGalR1/CHO cells was measured with flow cytometry. Shown in Figure 1C is the specific binding of F−Gal to rGalR1 receptor expressed in CHO cells. Nonlinear regression analysis yielded a $K_D$ of 49 ± 13 nM ($n = 3$), a high affinity comparable to that obtained in the intact cell binding assays shown in Figure 1B, and a $B_{max}$ of 10.1 ± 0.9 (arbitrary units, $n = 3$) (Figure 1C and Table 1). The best signal-to-noise ratio (N/S = total fluorescence/nonspecific fluorescence) was obtained as F−Gal approached 100 nM (N/S = 8.52, Figure 1C). Further increase of F−Gal resulted in an increase of both total and nonspecific binding and thus a decrease of signal-to-noise ratio (2.5 and 1.82 for F−Gal at 250 and 500 nM, respectively; Figure 1C). When parental CHO cells were incubated with F−Gal in the same concentration range, a curve identical to that of the nonspecific binding shown in Figure 1C was obtained (Figure 1C), indicating that the nonspecific binding consisted of binding of galanin and the fluorescein moiety of F−Gal to the plasma membrane, and that the 45-min postincubation with 5 $\mu$M unlabeled galanin completely removed the receptor-bound F−Gal on the cell surface; the remaining fluorescence represented only the nonspecific binding of F−Gal to the plasma membrane.

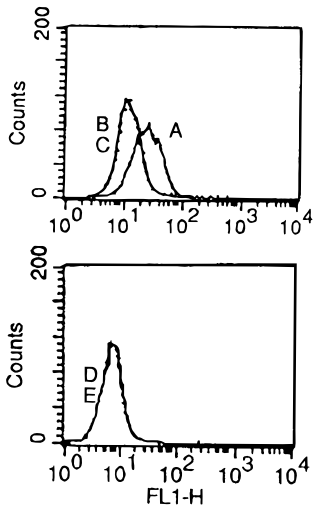


FIGURE 2: Histograms of F−Gal interaction with rGalR1/CHO and CHO cells. Flow cytometry was performed as described under Materials and Methods. The scans in the top panel represent total binding (A, unblocked sample), nonspecific binding (B, blocked sample in the presence of 5 $\mu$M unlabeled galanin) of F−Gal (100 nM) to rGalR1/CHO cells, and nonspecific binding of F−Gal (100 nM) to parental CHO cells (C, unblocked nonspecific sample). Note B and C are superimposable. The bottom panel contains autofluorescence of CHO (E) and rGalR1/CHO cells (D). Note these distributions are also superimposable. FL1-H and Counts represent fluorescence intensity and cell counts, respectively.

To illustrate the relative fluorescence of the total binding (unblocked sample), nonspecific binding (blocked sample) of F−Gal to rGalR1/CHO cells, and nonspecific binding of F−Gal to parental CHO cells (unblocked nonspecific sample) displayed in Figure 1C, Figure 2 shows the histograms for the fluorescence intensities of rGalR1/CHO incubated with 100 nM F−Gal in the absence and presence of 5 $\mu$M unlabeled galanin (Figure 2, scans A and B, respectively), that of CHO cells incubated with 100 nM F−Gal (Figure 2, scan C), and those of rGalR1/CHO and CHO incubated with no F−Gal (autofluorescence; Figure 2, scans D and E, respectively). Typical mean fluorescence intensities were 19.0, 8.5, and 7.0 for the scans A, B, and D, respectively. Since scans B and C were indistinguishable (Figures 2 and

1C), CHO cells incubated with F−Gal (C) were used as the blocked sample (B) in calculations for KI quenching as described below.

These data demonstrated that modification at G1 of galanin does not significantly affect the functions of galanin. High-affinity binding of rGalR1 has been retained in both F−Gal and biotinyl-galanin. There was, however, a small but consistent decrease in the affinity of these galanin analogues in binding rGalR1 as compared with native galanin (generally under 6-fold, Table 1). Since G1 of galanin is involved in galanin/receptor binding by formation of a hydrogen bond (*19*), the fluorescein moiety of F−Gal is most likely located at the ligand binding sites. The magnitude of affinity loss in the present studies indicates a decrease in binding energy smaller than that expected for loss of a hydrogen bond, suggesting a partial compensation by the addition of hydrophobic fluorescein or biotin to galanin. F−Gal and galanin activated rGalR1 at equal potency in inhibition of forskolin-stimulated intracellular cAMP, suggesting that both F−Gal and galanin possess a common active conformation when bound to rGalR1. Methylation of the N-terminus of galanin also preserved high-affinity binding to GalR1 (*20*), which is similar to those of galanin and high affinity analogues. The lower affinity/potency of galanin observed in the whole-cell assays (binding and cAMP) using PBS buffer (Table 1) than those seen in membrane binding assays (using only Tris-HCl buffer, low $Na^+$ concentration; Table 1) may result from the effect of $Na^+$ on reducing galanin binding to the receptor (*21*, *22*).

*Fluorescent Quenching of F−Gal by KI.* Fluorescence quenching experiments were employed to study the accessibility of the fluorescein moiety of F−Gal to the solvent-based collisional quencher KI. The fluorescence intensity of free F−Gal in PBS buffer, as measured spectroscopically, was readily quenched by KI in a dose-dependent manner (inset of Figure 3). Stern−Volmer analysis of the data using eq 1 gave a quenching constant ($K_q$) of 13.0 ± 3.6 $M^{-1}$ ($n$ = 2), indicating a collision-controlled bimolecular interaction between F−Gal and the quencher KI in solution. The degree of quenching also suggests that the fluorescein moiety in F−Gal is not protected by galanin. KI quenching of fluorescence of F−Gal bound to rGalR1/CHO cells was measured with flow cytometry. When F−Gal was bound to its receptor in rGalR1/CHO cells, substantially lower quenching was observed ($K_q$ = 0.04 ± 0.44 $M^{-1}$, $n$ = 3; Figure 3), indicating that the fluorescein moiety of F−Gal is well protected from the solvent when bound to the receptor. As a control, the KI quenching of F−FA, a dodecanoyl fatty acid with fluorescein linked to the polar headgroup, was measured in these cells. When F−FA is incorporated into cell membranes, the fluorescein group positions at the water/membrane interface (*23*). A $K_q$ of 2.53 ± 0.35 $M^{-1}$($n$ = 3) was obtained when the fluorescence of bound F−FA on CHO cells was quenched by KI (Figure 3), indicating that at the cell surface fluorescein is accessible to the solvent-based quencher, although the accessibility is reduced compared to that of free F−Gal in solution.

The hypothesis that the N-terminal portion of galanin is deeply buried in rGalR1 was further tested by using biotinyl-galanin in flow cytometry and radioligand binding assays. Like F−Gal, the biotin moiety of biotinyl-galanin was linked to the free amine group at the N-terminus of rat galanin and

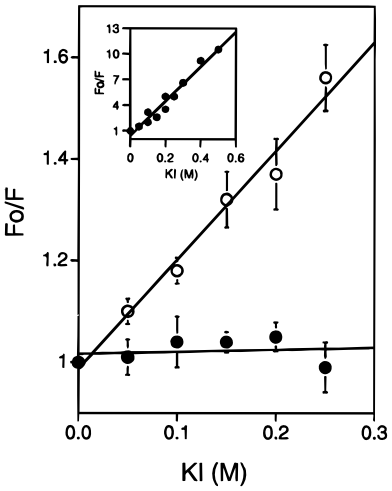


FIGURE 3: KI quenching of fluorescence of receptor-bound F−Gal. The fluorescent intensity of F−Gal (●) bound to rGalR1/CHO and F−FA (○) bound to CHO cells were measured with flow cytometry. F−Gal (100 nM) and F−FA (20 nM) were incubated with the cells for 45 min at 0 °C and fluorescence was measured at various concentrations of KI. $F_0$ and $F$ represent the mean fluorescent intensities of rGalR/CHO cells at [KI] = and > 0 M, respectively. The mean fluorescent intensities of blank samples (CHO cells incubated with 100 nM F−Gal) at appropriate [KI] were subtracted. Data represent mean ± SE, $n$ = 3. Inset, KI quenching of free F−Gal in buffer A ($n$ = 2). Background intensity at an appropriate KI concentration in buffer alone was subtracted.

did not significantly affect the high-affinity binding of galanin to rGalR1. In radioligand competition assays using $^{125}$I−Gal and membranes from rGalR1/CHO cells or COS-7 cells transiently transfected with rGalR1 cDNA, similar affinities were obtained for galanin and biotinyl-galanin (Table 1). When biotinyl-galanin was incubated with rGalR1/CHO cells followed by staining with fluorescein−streptavidin, no rGalR1/CHO-associated fluorescence from fluorescein−streptavidin was detected by flow cytometry (not shown), suggesting that the biotin moiety of biotinyl-galanin bound to the receptor was not exposed to interact with aqueous phase fluorescein-streptavidin. Radioligand competition assays were then performed to detect the biotinyl-galanin interaction with streptavidin. Binding of $^{125}$I-galanin (0.1 nM) to rGalR1 was competed with biotinyl-galanin in the presence and absence of fluorescein−streptavidin (Figure 4). In the absence of fluorescein−streptavidin (control), the $K_i$ of biotinyl-N-galanin for rGalR1 was 0.42 ± 0.09 nM ($n$ = 3). Mixing biotinyl-galanin with fluorescein−streptavidin (final concentration 1 $\mu$g/mL) prior to the radioligand binding resulted in a $K_i$ of 12.0 ± 3 nM ($n$ = 3), a decrease of affinity by 29-fold (Figure 4). In contrast, addition of fluorescein−streptavidin after incubation of biotinyl-galanin with rGalR1 resulted in identical affinity ($K_i$ = 0.52 ± 0.12 nM, $n$ = 3) to that of the control (Figure 4). The final concentration of fluorescein−streptavidin was 1:1000 dilution of original stock solution, equivalent of 70 nM biotin binding sites. The results demonstrate that the biotin moiety is not accessible to fluorescein−streptavidin only when biotinyl-galanin is bound to rGalR1.

The KI quenching and biotin/streptavidin interaction data have illustrated that the fluorescein moiety of receptor-bound F−Gal is almost completely protected from quenching by KI, an ionic species that partitions into the aqueous solvent phase ($K_q$ = 0.04 $M^{-1}$; Figure 3). Several lines of evidence

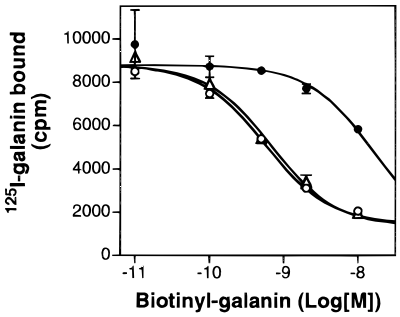


FIGURE 4: Interaction of biotinyl-galanin with rGalR1 receptor. Ten micrograms of CHO cell membrane containing rGalR1 was incubated for 1 h at room temperature with 0.1 nM $^{125}$I-galanin and various concentrations of biotinyl-N-galanin with addition of a 30-min postincubation with or without 1 $\mu$g/mL fluorescein−streptavidin. Symbols (mean ± SE, $n = 3$) are control (○), fluorescein-streptavidin mixed with biotinyl-galanin before adding into binding assays (●) and fluorescein-streptavidin present in postincubation (Δ). The curves indicate one-site fits of nonlinear regression analysis.

suggest that the ligand/receptor interaction is accommodated by a hydrophobic pocket in GalR1. (1) The two halves of galanin that form the horseshoe conformation are different in hydrophobicity; the N-terminal half (amino acids 1−16) capable of binding the receptor by itself is significantly more hydrophobic than the C-terminal portion (amino acids 17−29), which can be removed without significantly affecting the affinity of galanin (*19*). Ala-scanning substitution within residues 1−16 identified mostly hydrophobic residues (W2, T3, N5, Y9, L10, and L11) essential for receptor binding (40−400 less potency) (*19*). (2) Receptor mutagenesis studies of GalR1 have identified five amino acid residues important for galanin/receptor binding (*24*, *25*). Three of these residues, F115, F282, and H264, are located in the hydrophobic TMs. (3) The F−Gal/GalR1 interaction highly protected from KI quenching is in contrast to those of other peptide ligands and their GPCRs. A high degree of KI quenching was observed with fluorescein-labeled NK2 (neurokinin 2 receptor) peptide agonists AGO-2 and AGO-4 bound to the NK2 receptor ($K_q = 4.2-4.5$ $M^{-1}$) (*26*), fluorescein-substance P to the NK1 receptor (*27*), and fluorescein−glucagon to the glucagon receptor (*28*), all of which remained largely solvent-exposed when bound to their receptors. In contrast, a high degree of protection from the quenching was observed with small, hydrophobic molecule $\beta$-adrenergic receptor (AR) antagonist carazolol ($K_q = 0.19$ $M^{-1}$ by KI quenching), similar to that observed with F−Gal (Figure 3). Subsequent energy transfer measurements determined that carazozol is buried a minimum of 11 Å into the hydrophobic milieu of the $\beta$-AR (*29*). Therefore, the fluorescein moiety of F−Gal is likely located in the middle of the membrane, rendering the N-terminal half of galanin beneath the water−membrane interface.

*GalR1-Induced F−Gal Internalization.* The possibility of agonist-triggered internalization of F−Gal in rGalR1/CHO cells was assessed by measuring the kinetics of F−Gal association with cellular rGalR1 receptor by flow cytometry. Fluorescence for total binding, including the surface and internalized F−Gal, was determined in the absence of competing galanin in a 45-min postincubation. Fluorescence of internalized F−Gal was determined in the presence of competing galanin in the postincubation. The difference

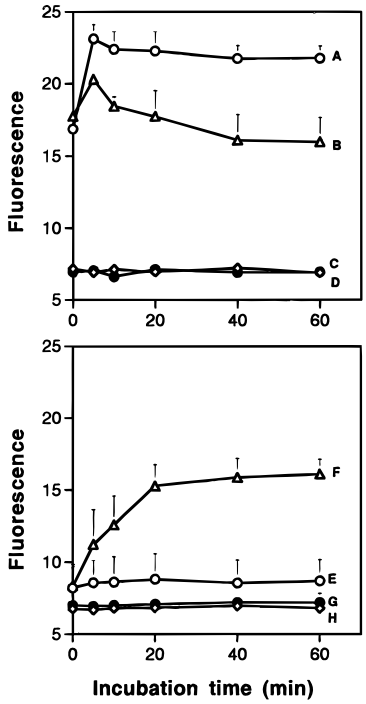


FIGURE 5: GalR1-mediated internalization of F−Gal into rGalR1/CHO cells. F−Gal (100 nM) was incubated with rGalR1/CHO or CHO cells in 100 $\mu$L of buffer C at 0 or 37 °C for the designated time. At the end of incubation, the stained cells were either incubated with 0.5 mL of buffer A containing either 0 $\mu$M (upper panel) or 5 $\mu$M unlabeled galanin (lower panel) at 0 °C for 45 min. The fluorescent intensities of the cells were measured by cell flow cytometry. The data represent mean fluorescent intensities of two independent experiments with the error bars denoting the range of the two values. The autofluorescence of the cells in the absence of F−Gal was 7.0 ± 1.7 ($n = 8$). The symbols denote CHO cells at 0 °C (●); CHO cells at 37 °C (◇), rGalR1/CHO cells incubated at 0 °C (○); and rGalR1/CHO cells at 37 °C (Δ).

between the total and internalized F−Gal represents the surface-bound F−Gal. The association of F−Gal was performed at two temperatures, 37 and 0 °C (ice water bath), to allow rGalR1 internalization at different rates.

Total binding of F−Gal to rGalR1/CHO cells at 0 °C rapidly reached a plateau ($t_{1/2} \ll 5$ min) and remained unchanged for up to 1 h (upper panel, Figure 5, curve A − curve C [A − C]). At 37 °C (B − D), the ligand binding also reached a comparable maximum level within 5 min but the initial peak was followed by a small decrease of the F−Gal intensity (curve B, Figure 5). The descending intensity reached steady state at ∼40 min ($t_{1/2} = \sim 20$ min), with a fluorescence intensity 61% that at 0 °C ([B − D]/[A − C] = 0.61; Figure 5). The data demonstrate that, at both temperatures, F−Gal quickly binds to rGalR1 with a similar maximum binding capacity and that binding of the ligand to GalR1 receptor at 37 °C triggered a loss of 39% of total ligand binding sites from cells within 60 min. At both temperatures, the association of F−Gal was best estimated to be $t_{1/2} < 0.5$ min as it was faster than the time of initial measurement (Figure 5, curves A and B at $t = \sim 0$ min).

In the presence of competing galanin in the postincubation, internalized F−Gal displayed a different pattern (lower panel, Figure 5). Minimal internalization of F−Gal occurred at 0 °C (Figure 5, E − G). Comparison of curves A and E indicates that the receptor-bound F−Gal at 0 °C was mainly on the cell surface, represented by the difference between

curves A and E ([(A − C) − (E − G)]/[A − C] = 0.89 at $t \geq 10$ min). When incubated at 37 °C, F−Gal underwent substantial internalization as evidenced by a rapid increase of the fluorescent intensity of internalized F−Gal, protected from subsequent competition with unlabeled galanin (Figure 5, curve F). The internalization proceeded rapidly at early time points ($t_{1/2} = \sim 10$ min) and reached a maximum in 20 min (curve F). Since [B − D] represents both surface and internalized F−Gal, the relative amount of internalized F−Gal over the total F−Gal can be expressed as

$$R = [(F - H) - (E - G)]/[B - D] \qquad (2)$$

*R* approached 62% at $t = 20$ min and 78% at $t \geq 40$ min. Because the rapid ($t_{1/2} = \sim 10$ min) and strikingly high degree (∼78%) of internalization of F−Gal was only observed with GalR1/CHO cells, not control cells, at only 37 °C, these results demonstrate that the internalization of F−Gal is mediated by rGalR1 in an energy-requiring process. After the binding of F−Gal to GalR1, the ligand/receptor complex may be intracellularly sequestered away from the plasma, which may (1) act as a negative feedback mechanism to prevent the receptor from being constantly activated by reducing the number of surface receptors that are responsive to ligand stimuli and (2) provide a mechanism to reduce the excessive amount of agonist that the cells are exposed to, as the receptor carries along the agonist molecules into the cells. Internalized F−Gal may be subject to intracellular degradation, as suggested by the loss of approximately $^1/_3$ of the cell-associated F−Gal [(A − B) in the upper panel, Figure 5]. Alternatively, the loss may result from acidic quenching of internalized F−Gal fluorescence in intracellular compartments. Correction of this type of loss for the internalization (*R* in eq 2) by adding (A − B) to terms F and B in eq 2 yielded 74% and 90% as the maximum possible internalization of F−Gal at $t = 20$ and ≥40 min, respectively. Thus, assuming various degrees of acidic quenching existed, F−Gal internalization could range between 62% and 74% at 20 min and between 78% and 90% at ≥40 min (Figure 5).

Since not all the G protein-coupled receptors are internalized upon ligand activation and the modification of galanin by fluorescein may potentially alter internalization properties, we confirmed the internalization results with radiolabeled galanin (Figure 6). When rGalR1/CHO cells were incubated with $^{125}$I-galanin (0.2 or 1 nM) at 0 °C followed by removal of surface GalR1-bound $^{125}$I-galanin, no internalization of the ligand was observed during the 60-min incubation period (Figure 6). In contrast, when the incubation was performed at 37 °C, internalization of the ligand, as indicated by a 2−3-fold increase of intracellular $^{125}$I-galanin at 60 min, was observed (Figure 6). When the same experiments were performed with CHO cells, no internalization was observed at either 0 or 37 °C (not shown), indicating again a GalR1-mediated internalization.

Although it is most likely that the absence of dissociation of F−Gal or $^{125}$I-galanin from the rGalR1/CHO cells represents internalization of the ligand, there is a possibility that ligand-activated cell surface rGalR1 receptors undergo an affinity change for F−Gal and $^{125}$I-galanin at 37 °C, which may interfere with the postincubation competition shown in Figures 5 and 6. However, compared to the rate of the affinity change (∼11 s for N-formylpeptide receptor) (*35*),

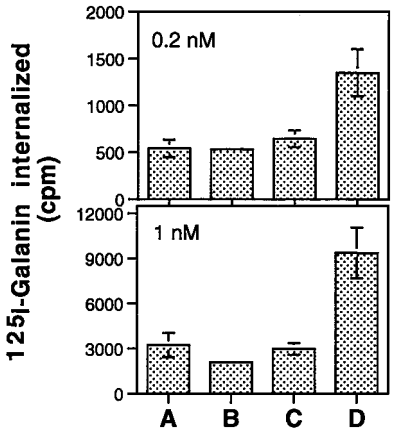


FIGURE 6: GalR1-mediated internalization of $^{125}$I-galanin into rGalR1/CHO cells. rGalR1/CHO cells were incubated with 0.2 nM (top) or 1 nM (bottom) $^{125}$I-galanin at 0 or 37 °C for 0 or 60 min in 200 μL of buffer C. At the end of incubation, 20 μL of 20 μM rat galanin was added and the mix was incubated for an additional 20 min at 0 °C. Internalized $^{125}$I-galanin was determined by filtering of the mix and scintillation counting of the filters as described in Materials and Methods. (A) 0 °C, 0 min; (B) 0 °C, 60 min; (C) 37 °C, 0 min; and (D) 37 °C, 60 min. Data represent mean ± SD ($n = 4$).

the internalization of the F−Gal/rGalR1 complex is slow (∼600 s, Figure 5), similar to the internalization of the fluorescent N-formyl peptide/receptor complex into the neutrophil (∼300 s) (*35*). These kinetic data suggest that the observed increased fluorescence of the uncompetable F-Gal or increased radioligand counts in rGalR1/CHO cells at 37 °C (Figures 5 and 6) resulted from internalization, not an affinity change of the rGalR1 receptor.

To explore the mechanism(s) of the GalR1-mediated internalization of F−Gal, several agents that may modulate internalization of GPCRs were used. In these experiments, internalized F−Gal accounted for 79% ± 7% of the total rGalR1-bound F−Gal (bars 2 and 3, Figure 7). Pretreatment of the GalR1/CHO cells for 30 min with 0.25 M sucrose, which disrupts the clathrin-mediated endocytic pathway, reduced 73.5% ± 5% ($n = 3$) of the internalized F−Gal in rGalR1/CHO cells (Figure 7). Hypertonic treatment of cells by addition of sucrose has been shown to inhibit receptor-mediated endocytosis by blocking the clathrin-coated pit formation (*30*). In contrast, pretreatment with GTP-γ-S (uncouples G protein from the receptor), chloroquine, or $NH_4$-Cl (neutralizes the acidic pH of endosomes and lysosomes) did not affect the internalization (Figure 7). Phenylarsine oxide, known as an endocytosis inhibitor that reacts specifically with vicinal sulfhydryls to form stable ring structures (*34*, *35*), did not affect the receptor-mediated internalization of F−Gal. In addition, treatment of the cells with okadaic acid, calphostin C, staurosporine, or OAG, known as the modulators of phosphatase, protein kinase C, and protein kinase A, respectively, had no substantial effect on the internalization. However, the lack of effects of the protein kinase modulators does not exclude potential roles of other kinases, such as GPCR kinases, in the internalization. Inhibition of F−Gal/rGalR1 internalization by hypertonic treatment and low temperature (Figures 5−7) indicates an active energy-consuming endocytosis that requires clathrin-coated pit formation. About $^1/_3$ of the fluorescent ligand enters the cells in hypertonic media (Figure 7), suggesting that this portion of the internalization may be mediated via

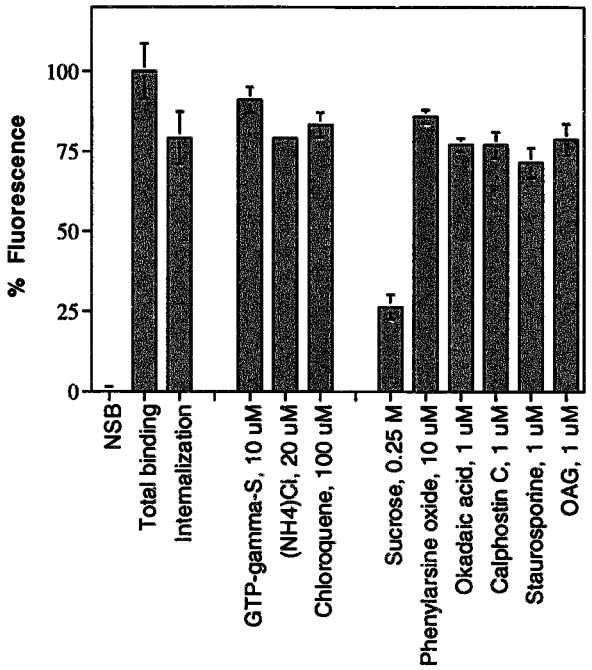


FIGURE 7: Effects of various agents on F−Gal-induced rapid internalization. rGalR1/CHO cells were treated with various agents at indicated concentrations for 30 min prior to the addition of agonist F−Gal. The cells were then incubated with F−Gal (100 nM) at 37 °C for 60 min. F−Gal bound on the cell surface rGalR1 receptor was removed by addition of 5 $\mu$M rat galanin followed by analysis with flow cytometry as described under Materials and Methods. The fluorescence of cells incubated in the absence of F−Gal (autofluorescence) was 11.1 ± 0.5, $n = 6$. The mean fluorescence of the cells without removal of the surface F−Gal is taken as the control (100% as total binding, fluorescence = 61.0 ± 2.8, $n = 6$) and that of cells coincubated with F−Gal and 5 $\mu$M unlabeled rat galanin (NSB) is taken as 0% (17.5 ± 0.9, $n = 3$). The data are representative of three independent experiments each performed in duplicate. NSB, nonspecific binding; GTP-gamma-S, GTP-$\gamma$-S; OAG, 1-oleoyl-2-acetyl-*sn*-glycerol.

a non-coated pit-mediated pathway, as has been observed with the cholecystokinin receptor, which is internalized by both the clathrin-coated and non-clathrin-coated pit-mediated pathways (*31*).

In conclusion, we have generated a novel, active fluorescent analogue of galanin and used it in flow cytometry to probe galanin/rGalR1 interaction and internalization of the galanin/rGalR1 complex from the plasma membrane into CHO cells. The studies have provided first evidence for the binding of galanin to a highly hydrophobic environment within the GalR1 receptor and evidence for a rapid and massive internalization of the galanin/rGalR1 complex, triggered by a high affinity ligand binding, primarily through an energy-requiring endocytic mechanism. The method of using sensitive flow cytometry in detection of ligand/receptor interaction and movement in cells that express only moderate levels of GalR1 avoided tedious overexpression and purification of the receptor for physical studies, which have been commonly performed in studies for other GPCRs.

## REFERENCES

1. Bartfai, T., Hokfelt, T., and Langel, U. (1993) *Crit. Rev. Neurobiol. 7*, 229−274.
2. Crawley, J. N. (1995) *Regul. Pept. 59*, 1−16.
3. Tatemoto, K., Rokaeus, A., Jornwall, H., McDonald, T. J., and Mutt, V. (1983) *FEBS Lett. 164*, 124−128.
4. Crawley, J. N., Austin, M. C., Fiske, S. M., Martin, B., Consolo, S., Berthold, M., Langel, U., Fisone, G., and Bartfai, T. (1990) *J. Neurosci. 10*, 3695−3700.
5. Ekblad, E., Hakanson, R., Sundler, F., and Wahlestedt, C. (1985) *Br. J. Pharmacol. 86*, 241−246.
6. Wiesenfeld-Hallin, Z., Villar, M. J., and Hokfelt, T. (1988) *Exp. Brain Res. 71*, 663−666.
7. Verge, V. M. K., Xu, X.-J., Langel, U., Hokfelt, T., Wiesenfeld, Z., and Bartfai, T. (1993) *Neurosci. Lett. 149*, 193−197.
8. Habert-Ortoli, E., Amiranoff, B., Loquet, I., Laburthe, M., and Mayaux, J. F. (1994) *Proc. Natl. Acad. Sci. U.S.A. 91*, 9780−9783.
9. Howard, A. D., Tan, C., Shiao, L.-L., Palyha, O. C., McKee, K. K., Weiger, D. H., Feighner, S. D., Cascieri, M. A., Smith, R. G., Van Der Ploeg, L. H. T., and Sullivan, K. A. (1997) *FEBS Lett. 405*, 285−290.
10. Wang, S., He, C., Hashemi, T., and Bayne, M. (1997) *J. Biol. Chem. 272*, 31949−31952.
11. Probst, W. C., Snyder, L. A., Schuster, D. I., Brosius, J., and Sealfon, S. C. (1992) *DNA Cell Biol. 11*, 1−20.
12. Wang, S., He, C., Maguire, M., Clemmons, A., Burrier, R., Guzzi, M., Strader, C., Parker, E., and Bayne, M. (1997) *FEBS Lett. 411*, 225−230.
13. Wang, S., Hashemi, T., He, C., Strader, C., and Bayne, M. (1997) *Mol Pharmacol. 52*, 337−343.
14. Morris, M. B., Ralston, G. B., Biden, T. J., Browne, C. L., King, G. F., and Iismaa, T. P. (1995) *Biochemistry 34*, 4538−4545.
15. Bartfai, T. (1995) in *Psychopharmacology: The Fourth Generation of Progress* (Bloom, F. E., and Kupfer, D. J., Eds.) pp 563−571, Raven Press, New York.
16. Schmid, I., Schmid, P., and Giorgi, J. V. (1988) *Cytometry 9*, 533−538.
17. Lakowicz, J. (1983) in *Principles of fluorescence spectroscopy* (Lakowicz, J., Ed.), pp 258−297, Plenum Press, New York.
18. Chen, R. F. (1969) *Arch. Biochem. Biophys. 133*, 265−276.
19. Land, T., Langel, U., Low, M., Berthold, M., Unden, A., and Bartfai, T. (1991) *Int. J. Pept. Protein Res. 38*, 267−272.
20. Rivera Baeza, C., Kask, K., Langel, U., Bartfai, T., and Unden, A. (1994) *Acta Chem. Scand. 48* (5), 434−438.
21. Walli, R., Schafer, H., C., M.-W., Paetzold, G., Nustede, R., and Schmidt, W. E. (1994) *J. Mol. Endocrinol. 13*, 347−356.
22. Amiranoff, B., Servin, A. L., Rouyer-Fessard, C., Couvineau, A., Tatemoto, K., and Laburthe, M. (1987) *Endocrinology 121*, 284−289.
23. Johnson, D., and Nuss, J. M. (1994) *Biochemistry 33*, 9070−9077.
24. Berthold, M., Kahl, U., Jureus, A., Kask, K., Nordvall, G., Langel, U., and Bartfai, T. (1997) *Eur. J. Biochem. 249*, 601−606.
25. Kask, K., Berthold, M., Kahl, U., Nordvall, G., and Bartfai, Y. (1996) *EMBO J. 15*, 236−244.
26. Turcatti, G., Vogel, H., and Collet, A. (1995) *Biochemistry 34*, 3972−3980.
27. Tota, M., Daniel, S., Sirotina, A., Mazina, K. E., Fong, T. M., Longmore, J., and Strader, C. D. (1994) *Biochemistry 33*, 13709−13086.
28. Tota, M. R., Xu, L., Sirotina, A., Strader, C. D., and Graziano, M. P. (1995) *J. Biol. Chem. 270*, 26466−26472.
29. Tota, M. R., and Strader, C. D. (1990) *J. Biol. Chem. 265*, 16891−16897.
30. Heuser, J. E., and Anderson, R. G. W. (1989) *J. Cell Biol. 108*, 389−400.
31. Roettger, B. F., Rentsch, R. U., Pinon, D., Holicky, E., Hadac, E., Larkin, J. M., and Miller, L. J. (1995) *J. Cell Biol. 128*, 1029−1041.
32. Cheng, Y., and Prusoff, W. H. (1973) *Biochem. Pharmacol. 22*, 3099−3108.
33. Klugerman, M. R. 1965 *J. Immunol. 95*, 1165−1173.
34. Webb, J. L. (1966) *Enzyme and Metabolic Inhibitors*, Vol. 3, Academic Press, New York.
35. Hoffman, J. F., Linderman, J. J., and Omann, G. M. (1996) *J. Biol. Chem. 271* (31), 18394−18404.

BI9731955